



# ALGEBRAIC ASPECTS OF MULTIPLE SCATTERING BY TWO PARALLEL CYLINDERS: CLASSIFICATION AND PHYSICAL INTERPRETATION OF SCATTERING RESONANCES

Y. DECANINI, A. FOLACCI, P. GABRIELLI AND J.-L. ROSSI

*URA 2053 CNRS, Systèmes Dynamiques Énergétiques et Mécaniques, Equipe  
Ondes et Acoustique, Université de Corse, Faculté des Sciences, BP 52, 20250  
Corte, France*

*(Received 24 September 1997, and in final form 20 July 1998)*

Acoustic scattering by a pair of identical parallel cylinders is studied by emphasizing the role of the symmetries of the scatterer. Incident and scattered fields are expanded over the different irreducible representations of  $C_{2v}$ , the symmetry group of the scatterer. Then, from the boundary conditions, one obtains an infinite set of four linear complex algebraic equations (each one associated with a representation) where the unknown coefficients of the scattered fields are uncoupled. This method significantly simplifies the numerical treatment of the problem. As a consequence, positions of the scatterer resonances are determined in the complex plane of the reduced frequency and a partial algebraic classification of the resonances is obtained for various boundary conditions (soft cylinders, hard cylinders and elastic cylinders immersed in water). A physical interpretation of certain resonances in terms of trapped geometrical paths is provided.

© 1999 Academic Press

## 1. INTRODUCTION

The study of acoustic scattering by a pair of identical parallel cylinders has been the subject of an intense activity during the last 40 years. The most popular approach to that physical problem is based on the techniques of multiple scattering. For a clear presentation of multiple scattering by two cylinders, this paper refers to the work of Young and Bertrand which simplifies and extends the important contributions of Twersky (see for example reference [1] and references therein). Curiously, the use of symmetries of the two-cylinder scatterer in order to simplify the multiple scattering formalism has never been considered in acoustics. By contrast, in quantum physics, symmetry considerations have been and are extensively used. See, for example, the book of Landau and Lifshitz [2] for applications in crystallography, in atomic and molecular physics, and for

recent applications in quantum chaos the papers of Gaspard and Rice [3] and Cvitanović and Eckhardt [4].

Symmetry considerations greatly simplify the mathematical analysis of scattering problems. Indeed, when one considers scattering by objects of simple shapes such as a cylinder (respectively a sphere), the invariance of the Helmholtz equation under rotations about the cylinder axis (respectively about the center of the sphere) leads to the search of mode solutions by separation of variables of the form  $f(r) \exp(im\theta)$  (respectively  $f(r)Y_{lm}(\theta, \varphi)$ ). This is directly linked to the following mathematical results: the  $(\exp(\pm im\theta))$ , with  $m$  fixed, form a basis for a two-dimensional irreducible representation of  $O(2)$ , the invariance group of the cylinder, (respectively the spherical harmonics  $Y_{lm}(\theta, \varphi)$ , with  $l$  fixed and  $m = -l, \dots, +l$ , form a basis for the  $2l + 1$ -dimensional irreducible representation of  $O(3)$ , the invariance group of the sphere). These mathematical considerations are implicitly used in the partial wave expansions of the incident and scattered fields.

In the two-cylinder scatterer case, the invariance of a single cylinder under the continuous group  $O(2)$  is broken, but the full system is however invariant under a finite group. Indeed, the geometry of the two-cylinder scatterer, as shown in Figure 1, is invariant under four symmetry transformations: (i)  $E$ , the identity transformation, (ii)  $C_2$ , the rotation through  $\pi$  about the  $Oz$  axis, (iii)  $\sigma_x$ , the mirror reflection in the plane  $Oxz$ , and (iv)  $\sigma_y$ , the mirror reflection in the plane  $Oyz$ . These four transformations form a finite group of order 4, labelled  $C_{2v}$  in the mathematical literature (see for example the book of Hamermesh [5]), which can be called the symmetry group of the scatterer. Four one-dimensional irreducible representations labelled  $A_1, A_2, B_1, B_2$  are associated with this symmetry group  $C_{2v}$  [5]. In the study of acoustic scattering by two identical parallel cylinders, it seems then natural to express the incident and scattered fields as sums of functions which act as basis functions in the four irreducible representations  $A_1, A_2, B_1, B_2$ .

In section 2, some properties of the irreducible representations  $A_1, A_2, B_1, B_2$  of the  $C_{2v}$  symmetry group are recalled, and the incident wave and the fields scattered by each cylinder over these four representations expanded. Then, from the boundary conditions at the surface of the cylinders, four systems of algebraic equations are obtained, each one associated with a given irreducible representation. The method used permits one to uncouple the pairs of unknown coefficients defining the scattered fields. The four systems of equations can then be solved numerically by truncation and used to obtain the scatterer resonances. In section 3, numerical results are presented for the positions of the scatterer resonances in the complex plane of the reduced frequency. Numerical calculations are performed for several boundary conditions: soft cylinders, hard cylinders and elastic cylinders immersed in water. Symmetry considerations permits one to partially classify the resonances. It may be necessary here to explicitly give the meaning of the term "resonances". In (classical or quantum) physics [6], a resonance is defined as a pole of the  $S$ -matrix associated with a given system. This definition, which differs from the usual terminology used by underwater acousticians is adopted. They only consider as resonances what

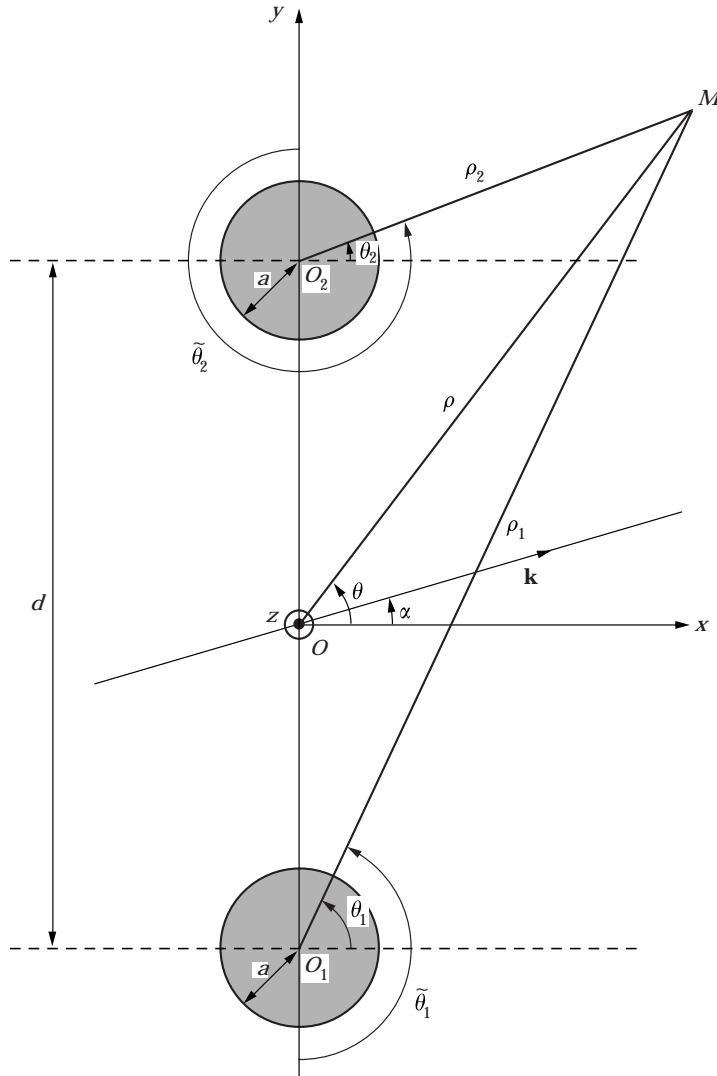


Figure 1. Two-cylinder co-ordinate systems

should be called elastic resonances and which are linked to the eigenfrequencies of the elastic vibrations of the scatterer. With the present definition, trapped mode wavenumbers are also included. In section 4, from the Sommerfeld–Watson transformation and asymptotic expansions of Bessel functions, certain sequences of resonances of interaction are associated with a geometrical path trapped between the two cylinders. In section 5, the interest of the method presented in this paper is emphasized and future extensions in the context of multiple scattering suggested. Furthermore, a direction of investigation is proposed in order to obtain a full classification of the two-cylinder scatterer resonances.

## 2. MATHEMATICAL FORMALISM

The scattering of a plane acoustic wave by a system of two identical and parallel cylinders of radius  $a$  is studied. The geometry of the problem as well as the notations used are shown in Figure 1. In particular,  $d$  denotes the distance between the axes of the two cylinders. Three cylindrical co-ordinate systems  $(\rho_1, \theta_1, z)$ ,  $(\rho_2, \theta_2, z)$ , and  $(\rho, \theta, z)$  are defined with respect to the axes of the cylinders and the symmetry axis  $Oz$  of the system. The incident propagation vector  $\mathbf{k}$  is perpendicular to the  $Oz$  axis and forms an angle  $\alpha$  with the  $Ox$  axis. The problem is then independent of the  $z$  co-ordinate. In the co-ordinate system  $(\rho, \theta)$  the incident wave reads

$$\Phi_{inc}(\rho, \theta) = e^{i\mathbf{k}\cdot\rho} = \sum_{m=-\infty}^{m=+\infty} i^m J_m(k\rho) e^{im(\theta-\alpha)}, \quad (1)$$

while the total scattered field from the two cylinders can be expressed in the form [1]

$$\Phi_s = \Phi_s^1(\rho_1, \theta_1) + \Phi_s^2(\rho_2, \theta_2), \quad (2)$$

with

$$\Phi_s^1(\rho_1, \theta_1) = \sum_{m=-\infty}^{m=+\infty} C_m^1 H_m^{(1)}(k\rho_1) e^{im\theta_1}, \quad (3)$$

$$\Phi_s^2(\rho_2, \theta_2) = \sum_{m=-\infty}^{m=+\infty} C_m^2 H_m^{(1)}(k\rho_2) e^{im\theta_2}. \quad (4)$$

Here and in the following the  $\exp(-i\omega t)$  time dependence is suppressed and  $J_m$  and  $H_m^{(1)}$  denote respectively ordinary Bessel functions of the first and third kinds [7]. Usually [1], this scattering problem is solved by applying boundary conditions for the total field  $\Phi_t = \Phi_{inc} + \Phi_s$  at the surface of each cylinder. By means of Graf's Addition Theorem [7], an infinite set of two linear, complex, algebraic equations is then obtained where the unknown coefficients  $C_m^1$  and  $C_m^2$  are coupled.

In order to solve this problem, a new method based on the use of the symmetries of the scatterer is proposed. As noted in section 1, the two-cylinder scatterer is invariant under four symmetry transformations: (i)  $E$ , the identity transformation, (ii)  $C_2$ , the rotation through  $\pi$  about the  $Oz$  axis, (iii)  $\sigma_x$ , the mirror reflection in the plane  $Oxz$ , and (iv)  $\sigma_y$ , the mirror reflection in the plane  $Oyz$ . These four transformations form the finite group of order 4, labelled  $\mathcal{C}_{2v}$ , which constitutes the symmetry group of the scatterer. The action of these transformations on an arbitrary function  $\Phi(\rho, \theta)$  is given by

$$(E\Phi)(\rho, \theta) = \Phi(\rho, \theta), \quad (5)$$

$$(C_2\Phi)(\rho, \theta) = \Phi(\rho, \pi + \theta), \quad (6)$$

TABLE 1  
Multiplication table of  $C_{2v}$

	$E$	$C_2$	$\sigma_x$	$\sigma_y$
$E$	$E$	$C_2$	$\sigma_x$	$\sigma_y$
$C_2$	$C_2$	$E$	$\sigma_y$	$\sigma_x$
$\sigma_x$	$\sigma_x$	$\sigma_y$	$E$	$C_2$
$\sigma_y$	$\sigma_y$	$\sigma_x$	$C_2$	$E$

$$(\sigma_x\Phi)(\rho, \theta) = \Phi(\rho, -\theta), \tag{7}$$

$$(\sigma_y\Phi)(\rho, \theta) = \Phi(\rho, \pi - \theta). \tag{8}$$

The multiplication table of  $C_{2v}$  is given in Table 1. That group can be represented by any set of four unitary matrices satisfying the multiplication table. If there exists a unitary transformation that transforms a given matrix representation into a diagonal or block-diagonal form, that representation is reducible. If no unitary transformation exists the representation is irreducible. Irreducible representations are the simplest representations: all others can be built up from them. Four one-dimensional irreducible representations labelled  $A_1, A_2, B_1, B_2$  are associated with this symmetry group  $C_{2v}$  [5]. In the representation  $A_1$  (respectively  $A_2, B_1$  and  $B_2$ ) the group elements  $E, C_2, \sigma_x$  and  $\sigma_y$  are represented by  $1 \times 1$  matrices given in the  $A_1$  (respectively  $A_2, B_1$  and  $B_2$ ) column of the character table (Table 2). The character table permits one to split any function  $\Phi$  as a sum of functions belonging to the four irreducible representations of  $C_{2v}$ . Indeed, one can write

$$\Phi = \Phi^{(A_1)} + \Phi^{(A_2)} + \Phi^{(B_1)} + \Phi^{(B_2)}, \tag{9}$$

with  $\Phi^{(A_1)}, \Phi^{(A_2)}, \Phi^{(B_1)}, \Phi^{(B_2)}$  satisfying

$$E\Phi^{(A_1)} = \Phi^{(A_1)}, \quad C_2\Phi^{(A_1)} = \Phi^{(A_1)}, \quad \sigma_x\Phi^{(A_1)} = \Phi^{(A_1)}, \quad \sigma_y\Phi^{(A_1)} = \Phi^{(A_1)}, \tag{10}$$

$$E\Phi^{(A_2)} = \Phi^{(A_2)}, \quad C_2\Phi^{(A_2)} = \Phi^{(A_2)}, \quad \sigma_x\Phi^{(A_2)} = -\Phi^{(A_2)}, \quad \sigma_y\Phi^{(A_2)} = -\Phi^{(A_2)}, \tag{11}$$

$$E\Phi^{(B_1)} = \Phi^{(B_1)}, \quad C_2\Phi^{(B_1)} = -\Phi^{(B_1)}, \quad \sigma_x\Phi^{(B_1)} = \Phi^{(B_1)}, \quad \sigma_y\Phi^{(B_1)} = -\Phi^{(B_1)}, \tag{12}$$

TABLE 2  
Character table of  $C_{2v}$ .

$C_{2v}$	$A_1$	$A_2$	$B_1$	$B_2$
$E$	1	1	1	1
$C_2$	1	1	-1	-1
$\sigma_x$	1	-1	1	-1
$\sigma_y$	1	-1	-1	1

$$E\Phi^{(B_2)} = \Phi^{(B_2)}, \quad C_2\Phi^{(B_2)} = -\Phi^{(B_2)}, \quad \sigma_x\Phi^{(B_2)} = -\Phi^{(B_2)}, \quad \sigma_y\Phi^{(B_2)} = \Phi^{(B_2)}. \quad (13)$$

It can be explicitly shown from the group table that  $\Phi^{(A_1)}$ ,  $\Phi^{(A_2)}$ ,  $\Phi^{(B_1)}$ ,  $\Phi^{(B_2)}$  given by

$$\Phi^{(A_1)} = \frac{1}{4}(E + C_2 + \sigma_x + \sigma_y)\Phi, \quad (14)$$

$$\Phi^{(A_2)} = \frac{1}{4}(E + C_2 - \sigma_x - \sigma_y)\Phi, \quad (15)$$

$$\Phi^{(B_1)} = \frac{1}{4}(E - C_2 + \sigma_x - \sigma_y)\Phi, \quad (16)$$

$$\Phi^{(B_2)} = \frac{1}{4}(E - C_2 - \sigma_x + \sigma_y)\Phi, \quad (17)$$

satisfy equations (10–13). Formally, it would be necessary to distinguish between  $E$ ,  $C_2$ ,  $\sigma_x$ ,  $\sigma_y$  considered as symmetry transformations acting in the plane  $Oxy$  and the associated operators appearing in equations (10–17) acting on functions defined on the  $Oxy$  plane. Here, in the case of the symmetry group  $C_{2v}$ , such a distinction is unnecessary.

The previous formalism admits a simple geometrical interpretation: if the modulus and the argument of  $\Phi^{(A_1)}$  (respectively  $\Phi^{(A_2)}$ ,  $\Phi^{(B_1)}$  and  $\Phi^{(B_2)}$ ) are given in the domain  $x \geq 0$  and  $y \geq 0$  of the  $Oxy$  plane, they are determined in the full  $Oxy$  plane from symmetry considerations based on equations (10–13) and (5–8).

The incident and scattered fields can now be expressed as sums of functions belonging in the four irreducible representations  $A_1$ ,  $A_2$ ,  $B_1$ ,  $B_2$ . For the incident field, the decomposition is obvious. By using equations (5–8) and (14–17), one obtains

$$\Phi_{inc}(\rho, \theta) = \Phi_{inc}^{(A_1)}(\rho, \theta) + \Phi_{inc}^{(A_2)}(\rho, \theta) + \Phi_{inc}^{(B_1)}(\rho, \theta) + \Phi_{inc}^{(B_2)}(\rho, \theta), \quad (18)$$

with

$$\Phi_{inc}^{(A_1)}(\rho, \theta) = \frac{1}{4} \sum_{m=-\infty}^{m=+\infty} \{(i^m + (-i)^m) e^{-im\alpha} + (i^m + (-i)^m) e^{im\alpha}\} J_m(k\rho) e^{im\theta}, \quad (19)$$

$$\Phi_{inc}^{(A_2)}(\rho, \theta) = \frac{1}{4} \sum_{m=-\infty}^{m=+\infty} \{(i^m + (-i)^m) e^{-im\alpha} - (i^m + (-i)^m) e^{im\alpha}\} J_m(k\rho) e^{im\theta}, \quad (20)$$

$$\Phi_{inc}^{(B_1)}(\rho, \theta) = \frac{1}{4} \sum_{m=-\infty}^{m=+\infty} \{(i^m - (-i)^m) e^{-im\alpha} + (i^m - (-i)^m) e^{im\alpha}\} J_m(k\rho) e^{im\theta}, \quad (21)$$

$$\Phi_{inc}^{(B_2)}(\rho, \theta) = \frac{1}{4} \sum_{m=-\infty}^{m=+\infty} \{(i^m - (-i)^m) e^{-im\alpha} - (i^m - (-i)^m) e^{im\alpha}\} J_m(k\rho) e^{im\theta}. \quad (22)$$

As far as the total scattered field is concerned, the decomposition is not so obvious and it is necessary to define new angular variables  $\tilde{\theta}_1$  and  $\tilde{\theta}_2$  (see Figure 1) which are more convenient to describe the action of the operators  $E$ ,  $C_2$ ,  $\sigma_x$  and  $\sigma_y$  on the total scattered field. They are linked to  $\theta_1$  and  $\theta_2$  by the following relations

$$\tilde{\theta}_1 = \theta_1 + \frac{\pi}{2} \quad \text{and} \quad \tilde{\theta}_2 = \theta_2 - \frac{\pi}{2}. \quad (23)$$

In this new set of variables, the total scattered field reads

$$\Phi_s = \Phi_s^1(\rho_1, \tilde{\theta}_1) + \Phi_s^2(\rho_2, \tilde{\theta}_2), \quad (24)$$

with

$$\Phi_s^1(\rho_1, \tilde{\theta}_1) = \sum_{m=-\infty}^{m=+\infty} \tilde{C}_m^1 H_m^{(1)}(k\rho_1) e^{im\tilde{\theta}_1}, \quad (25)$$

$$\Phi_s^2(\rho_2, \tilde{\theta}_2) = \sum_{m=-\infty}^{m=+\infty} \tilde{C}_m^2 H_m^{(1)}(k\rho_2) e^{im\tilde{\theta}_2}. \quad (26)$$

The new scattering coefficients  $\tilde{C}_m^i$  are given in terms of the previous ones by

$$\tilde{C}_m^1 = C_m^1 i^{-m} \quad \text{and} \quad \tilde{C}_m^2 = C_m^2 i^m. \quad (27)$$

The action of  $E$ ,  $C_2$ ,  $\sigma_x$  and  $\sigma_y$  on  $\Phi_s$  is then expressed in the form

$$E\Phi_s = \sum_{m=-\infty}^{m=+\infty} \tilde{C}_m^1 H_m^{(1)}(k\rho_1) e^{im\tilde{\theta}_1} + \sum_{m=-\infty}^{m=+\infty} \tilde{C}_m^2 H_m^{(1)}(k\rho_2) e^{im\tilde{\theta}_2}, \quad (28)$$

$$C_2\Phi_s = \sum_{m=-\infty}^{m=+\infty} \tilde{C}_m^2 H_m^{(1)}(k\rho_1) e^{im\tilde{\theta}_1} + \sum_{m=-\infty}^{m=+\infty} \tilde{C}_m^1 H_m^{(1)}(k\rho_2) e^{im\tilde{\theta}_2}, \quad (29)$$

$$\sigma_x\Phi_s = \sum_{m=-\infty}^{m=+\infty} (-1)^m \tilde{C}_{-m}^2 H_m^{(1)}(k\rho_1) e^{im\tilde{\theta}_1} + \sum_{m=-\infty}^{m=+\infty} (-1)^m \tilde{C}_{-m}^1 H_m^{(1)}(k\rho_2) e^{im\tilde{\theta}_2}, \quad (30)$$

$$\sigma_y\Phi_s = \sum_{m=-\infty}^{m=+\infty} (-1)^m \tilde{C}_{-m}^1 H_m^{(1)}(k\rho_1) e^{im\tilde{\theta}_1} + \sum_{m=-\infty}^{m=+\infty} (-1)^m \tilde{C}_{-m}^2 H_m^{(1)}(k\rho_2) e^{im\tilde{\theta}_2}. \quad (31)$$

From equations (10–13) and equations (28–31), one can write

$$\Phi_s = \Phi_s^{(A_1)} + \Phi_s^{(A_2)} + \Phi_s^{(B_1)} + \Phi_s^{(B_2)}, \quad (32)$$

with

$$\Phi_s^{(A_1)} = \sum_{m=-\infty}^{m=+\infty} \tilde{C}_m^{(A_1)} H_m^{(1)}(k\rho_1) e^{im\tilde{\theta}_1} + \sum_{m=-\infty}^{m=+\infty} \tilde{C}_m^{(A_1)} H_m^{(1)}(k\rho_2) e^{im\tilde{\theta}_2}, \quad (33)$$

$$\Phi_s^{(A_2)} = \sum_{m=-\infty}^{m=+\infty} \tilde{C}_m^{(A_2)} H_m^{(1)}(k\rho_1) e^{im\tilde{\theta}_1} + \sum_{m=-\infty}^{m=+\infty} \tilde{C}_m^{(A_2)} H_m^{(1)}(k\rho_2) e^{im\tilde{\theta}_2}, \quad (34)$$

$$\Phi_s^{(B_1)} = \sum_{m=-\infty}^{m=+\infty} \tilde{C}_m^{(B_1)} H_m^{(1)}(k\rho_1) e^{im\tilde{\theta}_1} - \sum_{m=-\infty}^{m=-\infty} \tilde{C}_m^{(B_1)} H_m^{(1)}(k\rho_2) e^{im\tilde{\theta}_2}, \quad (35)$$

$$\Phi_s^{(B_2)} = \sum_{m=-\infty}^{m=+\infty} \tilde{C}_m^{(B_2)} H_m^{(1)}(k\rho_1) e^{im\tilde{\theta}_1} - \sum_{m=-\infty}^{m=-\infty} \tilde{C}_m^{(B_2)} H_m^{(1)}(k\rho_2) e^{im\tilde{\theta}_2}. \quad (36)$$

Here the new scattering coefficients  $\tilde{C}_m^{(A_1)}$ ,  $\tilde{C}_m^{(A_2)}$ ,  $\tilde{C}_m^{(B_1)}$  and  $\tilde{C}_m^{(B_2)}$  must satisfy

$$\tilde{C}_{-m}^{(A_1)} = (-1)^m \tilde{C}_m^{(A_1)}, \quad \tilde{C}_{-m}^{(A_2)} = -(-1)^m \tilde{C}_m^{(A_2)}, \quad (37)$$

$$\tilde{C}_{-m}^{(B_1)} = -(-1)^m \tilde{C}_m^{(B_1)}, \quad \tilde{C}_{-m}^{(B_2)} = (-1)^m \tilde{C}_m^{(B_2)}. \quad (38)$$

The unknown coefficients  $\tilde{C}_m^{(A_1)}$ ,  $\tilde{C}_m^{(A_2)}$ ,  $\tilde{C}_m^{(B_1)}$  and  $\tilde{C}_m^{(B_2)}$  can be now determined from the boundary conditions at the surface of the cylinders. In fact, because we have taken into account the symmetries of the scatterer, it is enough to apply boundary conditions at the surface of only one cylinder. Moreover, boundary conditions are separately written in the four representations. For example, in the case of Dirichlet boundary conditions (soft cylinders), one can write

$$(\Phi_{inc}^{(A_1)} + \Phi_s^{(A_1)})_{\rho_2=a} = 0, \quad (\Phi_{inc}^{(A_2)} + \Phi_s^{(A_2)})_{\rho_2=a} = 0, \quad (39, 40)$$

$$(\Phi_{inc}^{(B_1)} + \Phi_s^{(B_1)})_{\rho_2=a} = 0, \quad (\Phi_{inc}^{(B_2)} + \Phi_s^{(B_2)})_{\rho_2=a} = 0. \quad (41, 42)$$

From equations (19–22), (33–38), and from Graf's Addition Theorems

$$J_m(k\rho) e^{im\theta} = \sum_{p=-\infty}^{p=+\infty} i^{m-p} J_{m-p}\left(\frac{kd}{2}\right) J_p(k\rho_2) e^{ip\theta_2}, \quad (43)$$

$$H_m^{(1)}(k\rho_1) e^{im\theta_1} = \sum_{p=-\infty}^{p=+\infty} i^{m-p} H_{m-p}^{(1)}(kd) J_p(k\rho_2) e^{ip\theta_2}, \quad (44)$$

which permit one to express all the fields in the co-ordinate system  $(\rho_2, \theta_2)$ , equations (39–42) respectively read

$$\sum_{p=0}^{p=+\infty} M_{mp}^{(A_1)} \tilde{C}_p^{(A_1)} = \alpha_m^{(A_1)} S_m(ka), \quad \text{for } m \geq 0, \quad (45)$$

$$\sum_{p=1}^{p=+\infty} M_{mp}^{(A_2)} \tilde{C}_p^{(A_2)} = \alpha_m^{(A_2)} S_m(ka), \quad \text{for } m \geq 1, \quad (46)$$



$$\sum_{p=1}^{p=+\infty} M_{mp}^{(B_1)} \tilde{C}_p^{(B_1)} = -\alpha_m^{(B_1)} S_m(ka), \quad \text{for } m \geq 1, \quad (47)$$

$$\sum_{p=0}^{p=+\infty} M_{mp}^{(B_2)} \tilde{C}_p^{(B_2)} = -\alpha_m^{(B_2)} S_m(ka), \quad \text{for } m \geq 0, \quad (48)$$

where the matrices  $M_{mp}^{(A_1)}$ ,  $M_{mp}^{(A_2)}$ ,  $M_{mp}^{(B_1)}$  and  $M_{mp}^{(B_2)}$  are given by

$$M_{mp}^{(A_1)} = \delta_{mp} - \frac{\gamma_p}{2} (-1)^m [\mathbf{H}_{m-p}^{(1)}(kd) + (-1)^p \mathbf{H}_{m+p}^{(1)}(kd)] S_m(ka), \quad (49)$$

$$M_{mp}^{(A_2)} = \delta_{mp} - (-1)^m [\mathbf{H}_{m-p}^{(1)}(kd) - (-1)^p \mathbf{H}_{m+p}^{(1)}(kd)] S_m(ka), \quad (50)$$

$$M_{mp}^{(B_1)} = \delta_{mp} + (-1)^m [\mathbf{H}_{m-p}^{(1)}(kd) - (-1)^p \mathbf{H}_{m+p}^{(1)}(kd)] S_m(ka), \quad (51)$$

$$M_{mp}^{(B_2)} = \delta_{mp} + \frac{\gamma_p}{2} (-1)^m [\mathbf{H}_{m-p}^{(1)}(kd) + (-1)^p \mathbf{H}_{m+p}^{(1)}(kd)] S_m(ka). \quad (52)$$

Here  $\gamma_p$  denotes the Neumann factor given by  $\gamma_0 = 1$  and  $\gamma_p = 2(p > 0)$ . The vector  $\mathbf{S}_m(ka)$ , which includes Dirichlet boundary conditions is given by

$$\mathbf{S}_m(ka) = -\frac{\mathbf{J}_m(ka)}{\mathbf{H}_m^{(1)}(ka)}, \quad (53)$$

while the vectors  $\alpha_m^{(A_1)}$ ,  $\alpha_m^{(A_2)}$ ,  $\alpha_m^{(B_1)}$  and  $\alpha_m^{(B_2)}$ , which are directly linked to the incident wave, are written as

$$\alpha_m^{(A_1)} = \frac{1}{4} [e^{im\alpha} + (-1)^m e^{-im\alpha}] e^{i\frac{kd}{2}\sin\alpha} + \frac{1}{4} [e^{-im\alpha} + (-1)^m e^{im\alpha}] e^{i\frac{kd}{2}\sin\alpha}, \quad (54)$$

$$\alpha_m^{(A_2)} = -\frac{1}{4} [e^{im\alpha} - (-1)^m e^{-im\alpha}] e^{i\frac{kd}{2}\sin\alpha} + \frac{1}{4} [e^{-im\alpha} - (-1)^m e^{im\alpha}] e^{i\frac{kd}{2}\sin\alpha}, \quad (55)$$

$$\alpha_m^{(B_1)} = -\frac{1}{4} [e^{im\alpha} - (-1)^m e^{-im\alpha}] e^{i\frac{kd}{2}\sin\alpha} - \frac{1}{4} [e^{-im\alpha} - (-1)^m e^{im\alpha}] e^{i\frac{kd}{2}\sin\alpha}, \quad (56)$$

$$\alpha_m^{(B_2)} = \frac{1}{4} [e^{im\alpha} + (-1)^m e^{-im\alpha}] e^{i\frac{kd}{2}\sin\alpha} - \frac{1}{4} [e^{-im\alpha} + (-1)^m e^{im\alpha}] e^{i\frac{kd}{2}\sin\alpha}. \quad (57)$$

Our algebraic approach developed for soft cylinders is still valid for more general boundary conditions. The scattering problem remains governed by equations (45–52) and equations (54–57). It is only necessary to change the vector  $\mathbf{S}_m(ka)$  in order to take into account the particular boundary conditions. In the case of Neumann boundary conditions (rigid cylinders), the vanishing of the normal derivative of the total field yields

$$S_m(ka) = -\frac{J'_m(ka)}{H'_m^{(1)}(ka)}. \quad (58)$$

For two elastic cylinders immersed in water, one obtains

$$S_m(ka) = \frac{D_m^{[1]}(ka)}{D_m(ka)} \quad (59)$$

from the continuity of normal displacements and stress continuity relations. Here  $D_m^{[1]}$  and  $D_m$  are the usual determinants of third rank with coefficients depending on the longitudinal and transverse velocities in the solid and the sound velocity in the liquid [8, 9].

It should be noted that the scattering of a plane acoustic wave by a system of two identical and parallel cylinders reduces to the solution of equations (45–48), an infinite set of four systems of algebraic equations, each one associated with a given irreducible representation. The unknown coefficients defining the scattered fields are uncoupled. The disappearance of a coupling is due to the symmetry considerations and greatly simplifies the treatment of the problem: the matrices  $M^{(A_1)}$ ,  $M^{(A_2)}$ ,  $M^{(B_1)}$  and  $M^{(B_2)}$  involved in calculations are better conditioned than those corresponding to the associated coupled problem. Indeed, the former can be considered as square roots of the latter. The four systems of equations can then be numerically solved by truncation and used to obtain the far field form function [10] of the system for various angles of incidence  $\alpha$ , angles of scattering  $\theta$  and separation distances  $d$ .

From now on, interest is focused on the resonances of the two-cylinder scatterer. The scattering resonances are the poles of the coefficients  $\tilde{C}_p^{(A_1)}$ ,  $\tilde{C}_p^{(A_2)}$ ,  $\tilde{C}_p^{(B_1)}$  and  $\tilde{C}_p^{(B_2)}$ . They can be determined by searching the zeros of  $\det M^{(A_1)}$ ,  $\det M^{(A_2)}$ ,  $\det M^{(B_1)}$  and  $\det M^{(B_2)}$  in the complex  $ka$ -plane and they are then naturally classified according to the irreducible representations  $A_1$ ,  $A_2$ ,  $B_1$  and  $B_2$ .

### 3. NUMERICAL RESULTS AND DISCUSSION

Numerical calculations of the zeros of  $\det M^{(A_1)}$ ,  $\det M^{(A_2)}$ ,  $\det M^{(B_1)}$  and  $\det M^{(B_2)}$  have been performed, for the separation distance  $d = 6a$  by replacing the infinite matrices  $M^{(A_1)}$ ,  $M^{(A_2)}$ ,  $M^{(B_1)}$  and  $M^{(B_2)}$  by associated matrices of rank  $N$ , with

$$N = \sup(8, [ka + 4(ka)^{1/3} + 1]). \quad (60)$$

The above truncation order  $N$  has been chosen from the numerical discussions of Young and Bertrand [1] and Nussenzweig [11], and it has been numerically tested. Positions of the scattering resonances are determined in the complex  $ka$ -plane by using the “argument principle” [12]: the integral

$$\frac{1}{2i\pi} \oint_{\gamma} \frac{d}{dka} (\ln \det M) dka \quad (61)$$

along the closed contour  $\zeta$  provides the difference between the number of zeros (with their multiplicities) of  $\det M$  and the number of its poles (with their multiplicities) lying in the enclosed region. The complex  $ka$ -plane is scanned in order to isolate all the zeros. It should be noted that such a process is greatly improved as a consequence of the present algebraic study which permits one to divide the work into four independent parts. Then the integral

$$\frac{1}{2i\pi} \oint_{\zeta} ka \frac{d}{dka} (\ln \det M) dka \tag{62}$$

permits one to calculate the co-ordinates of the zeros isolated in the enclosed region. Positions of the scattering resonances have been determined for the restricted domain  $0 \leq \text{Re } ka \leq 26$  and  $-1.8 \leq \text{Im } ka \leq 0$ . For larger reduced frequencies the computation of resonances becomes a time-consuming task. Moreover, such a choice is suitable for a future comparison between the exact positions of resonances and those calculated from a ray theory approximation.

Figure 2 (and respectively Figure 3) presents the positions of the resonances for Dirichlet (and respectively Neumann) boundary conditions. Resonances are distributed along certain curves of the complex  $ka$ -plane. A physical interpretation of these different curves by the phase-matching of geometrical and surface waves along closed paths seems possible. For example, in the next

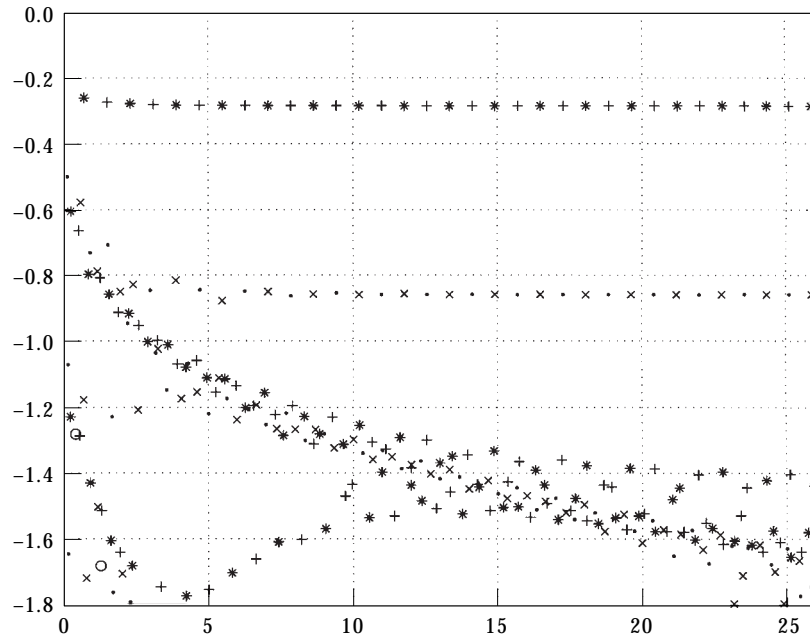


Figure 2. Location of the scattering resonances in the complex  $ka$ -plane. (Two soft cylinders, separation distance  $d = 6a$ .) Resonances corresponding to one single isolated cylinder are represented by open circles ( $\circ$ ). Resonances of the  $A_1$  representation are denoted by (\*), resonances of the  $A_2$  representation are denoted by ( $\cdot$ ), resonances of the  $B_1$  representation are denoted by ( $\times$ ), resonances of the  $B_2$  representation are denoted by (+).

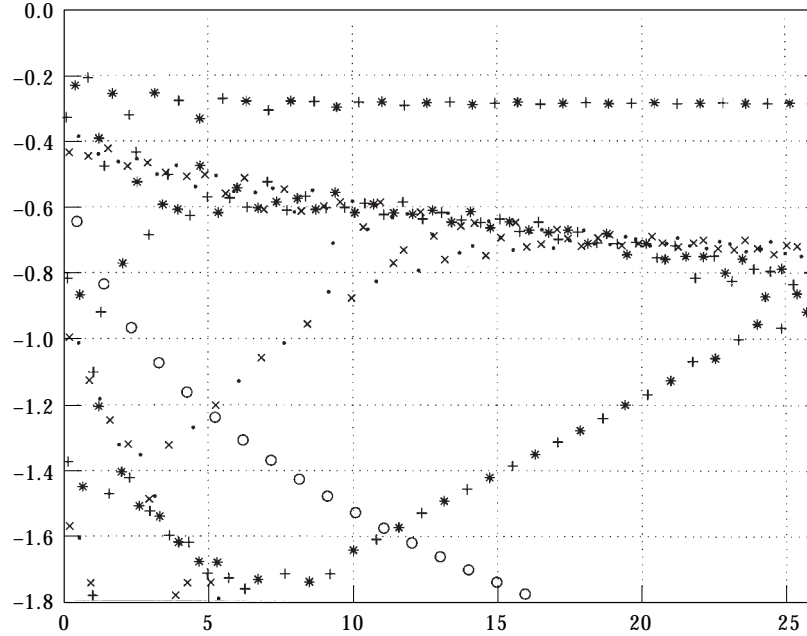


Figure 3. Location of the scattering resonances in the complex  $ka$ -plane. (Two rigid cylinders, separation distance  $d = 6a$ .) Resonances corresponding to one single isolated cylinder are represented by open circles ( $\circ$ ). Resonances of the  $A_1$  representation are denoted by (\*), resonances of the  $A_2$  representation are denoted by ( $\cdot$ ), resonances of the  $B_1$  representation are denoted by ( $\times$ ), resonances of the  $B_2$  representation are denoted by ( $+$ ).

section, is provided a physical interpretation for the resonances lying on the lines close to the real  $ka$ -axis.

Figure 4 (and respectively Figure 5) presents the positions of the resonances for two stainless steel (and respectively tungsten carbide) cylinders immersed in water. The computations were carried out for the following parameters: water ( $\rho_0 = 1 \text{ g cm}^{-3}$ ,  $v = 1480 \text{ m s}^{-1}$ ), stainless steel ( $\rho_0 = 7.98 \text{ g cm}^{-3}$ ,  $v_l = 5894 \text{ m s}^{-1}$ ,  $v_t = 3093 \text{ m s}^{-1}$ ), and tungsten carbide ( $\rho_0 = 13.80 \text{ g cm}^{-3}$ ,  $v_l = 6860 \text{ m s}^{-1}$ ,  $v_t = 4185 \text{ m s}^{-1}$ ). Far from the real  $ka$ -axis, the distribution of resonances is very close to the distribution corresponding to rigid cylinders. By contrast, for  $-0.4 \lesssim \text{Im } ka \lesssim 0$ , new features occur. All the resonances generated on a single isolated cylinder by the Rayleigh surface wave and the Brekhovskikh surface waves (whispering gallery surface waves) disappear because of the interactions between the two cylinders. They are split up into four new distinct resonances, each one corresponding to an irreducible representation of  $\mathcal{C}_{2v}$ .

#### 4. PHYSICAL INTERPRETATION OF RESONANCES

By generalizing the approach developed by Wirzba, [13] the resonances lying on the lines close to the real  $ka$ -axis can be associated with the geometrical path plotted in Figure 6. The characteristic equations  $\det M^{(A_1)} = 0$ ,  $\det M^{(A_2)} = 0$ ,

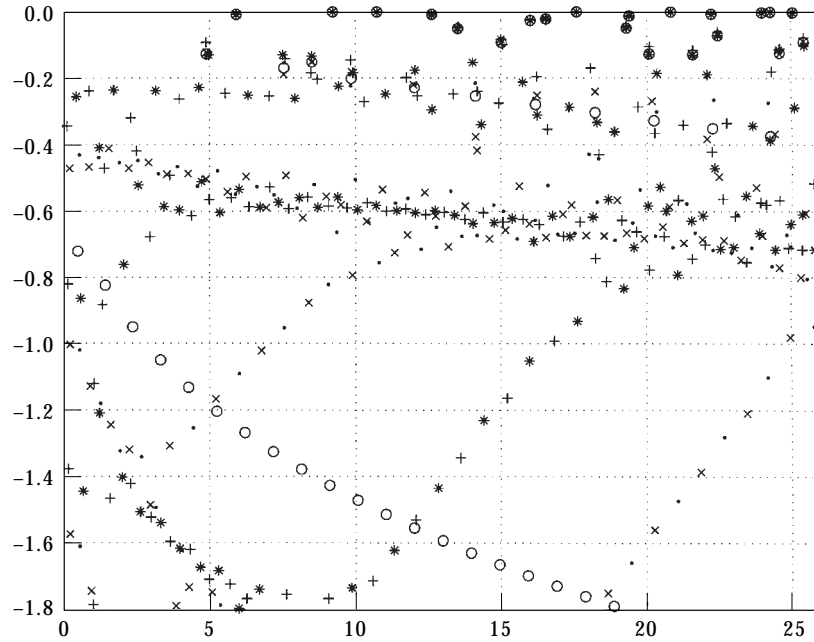


Figure 4. Location of the scattering resonances in the complex  $ka$ -plane. (Two stainless steel cylinders immersed in water, separation distance  $d = 6a$ .) Resonances corresponding to one single isolated cylinder are represented by open circles ( $\circ$ ). Resonances of the  $A_1$  representation are denoted by ( $*$ ), resonances of the  $A_2$  representation are denoted by ( $\cdot$ ), resonances of the  $B_1$  representation are denoted by ( $\times$ ), resonances of the  $B_2$  representation are denoted by ( $+$ ).

$\det M^{(B_1)} = 0$  and  $\det M^{(B_2)} = 0$  which respectively provide the locations of the  $A_1$ ,  $A_2$ ,  $B_1$  and  $B_2$  resonances in the complex  $ka$ -plane can be approximated for high frequencies by

$$1 - \frac{1}{2} \sum_{m=0}^{m=+\infty} \gamma_m (-1)^m S_m(ka) [H_0^{(1)}(kd) + (-1)^m H_{2m}^{(1)}(kd)] = 0 \quad \text{for } A_1 \text{ resonances,} \tag{63}$$

$$1 - \sum_{m=1}^{m=+\infty} (-1)^m S_m(ka) [H_0^{(1)}(kd) - (-1)^m H_{2m}^{(1)}(kd)] = 0 \quad \text{for } A_2 \text{ resonances,} \tag{64}$$

$$1 + \sum_{m=1}^{m=+\infty} (-1)^m S_m(ka) [H_0^{(1)}(kd) - (-1)^m H_{2m}^{(1)}(kd)] = 0 \quad \text{for } B_1 \text{ resonances,} \tag{65}$$

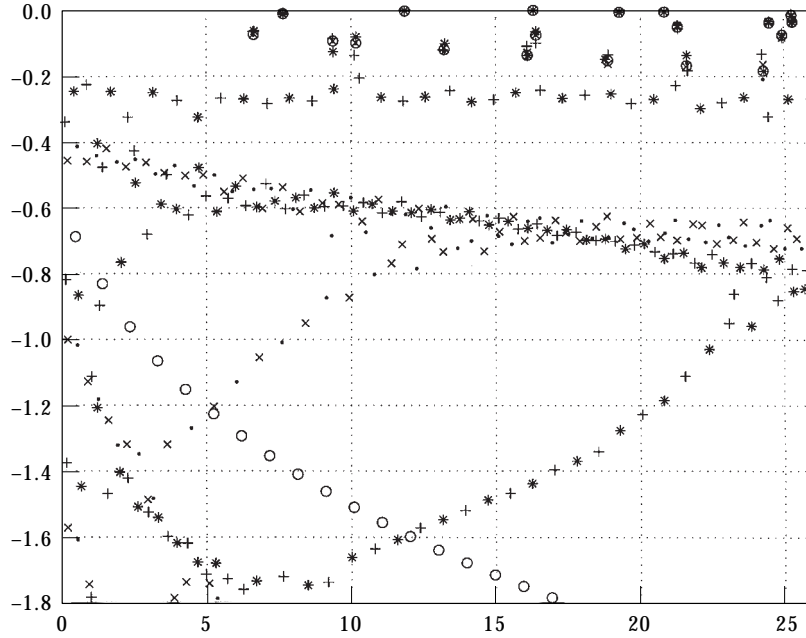


Figure 5. Location of the scattering resonances in the complex  $ka$ -plane. (Two tungsten carbide cylinders immersed in water, separation distance  $d = 6a$ .) Resonances corresponding to one single isolated cylinder are represented by open circles (O). Resonances of the  $A_1$  representation are denoted by (\*), resonances of the  $A_2$  representation are denoted by (·), resonances of the  $B_1$  representation are denoted by (x), resonances of the  $B_2$  representation are denoted by (+).

$$1 + \frac{1}{2} \sum_{m=0}^{m=+\infty} \gamma_m (-1)^m S_m(ka) [H_0^{(1)}(kd) + (-1)^m H_{2m}^{(1)}(kd)] = 0 \quad \text{for } B_2 \text{ resonances.} \tag{66}$$

The previous equations are directly obtained from the approximation  $\det(I + A) \sim 1 + \text{Tr } A$  which is a consequence of the expansion

$$\det(I + A) = \exp[\text{Tr} \ln(I + A)] = 1 + \text{Tr } A - \frac{1}{2} [\text{Tr } A^2 - (\text{Tr } A)^2] + \dots \tag{67}$$

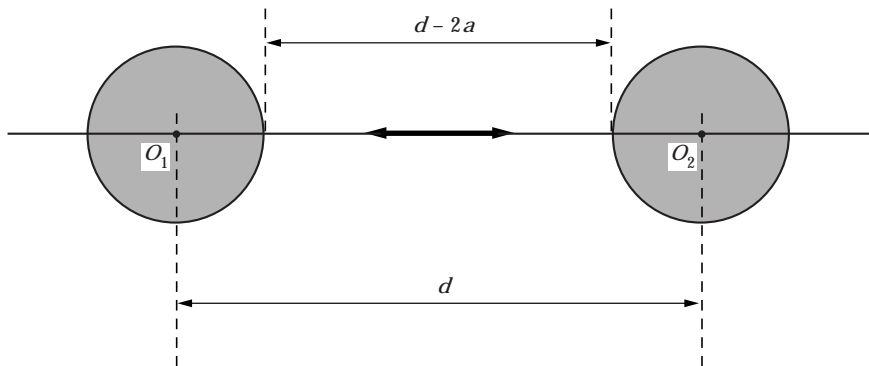


Figure 6. The closed geometrical path in the two-cylinder scattering problem.

First consider the partial wave series in equation (63)

$$\frac{1}{2} \sum_{m=0}^{m=+\infty} \gamma_m (-1)^m S_m(ka) [H_0^{(1)}(kd) + (-1)^m H_{2m}^{(1)}(kd)]. \tag{68}$$

By using the usual Watson transformation [14], it can be converted into the contour integral

$$\frac{i}{2} P \int_C S_\nu(ka) [e^{i\nu\pi} H_0^{(1)}(kd) + H_{2\nu}^{(1)}(kd)] \frac{\cos(\nu\pi)}{\sin(\nu\pi)} d\nu, \tag{69}$$

where  $S_\nu(ka)$  and  $H_{2\nu}^{(1)}(kd)$  are analytic functions in the complex  $\nu$ -plane, interpolating the numbers  $S_m(ka)$  and  $H_{2m}^{(1)}(kd)$ . Here the contour  $C$  encircles the real positive axis in the clockwise sense and  $P$  stands for Cauchy principal value at the origin. The deformation of the contour  $C$  away from the real positive axis permits one to extract from equation (69) the purely geometrical contribution (here surface wave contributions are not taken into account)

$$\frac{1}{4} \int_{C_s} \frac{H_\nu^{(2)}(ka)}{H_\nu^{(1)}(ka)} R_\nu [H_0^{(1)}(kd) e^{i\nu\pi} + H_{2\nu}^{(1)}(kd)] d\nu. \tag{70}$$

Here  $R_\nu$  denotes the direct reflection coefficient from the scatterer surface. Transmitted waves and internal reflected waves have been neglected in the Debye expansion [15, 16], so it will be assumed in what follows that  $R_\nu$  does not depend on  $ka$ . The contour  $C_s$  is described in Figure 7. It surrounds the poles of  $S_\nu(ka)$  and can be continuously deformed in order to evaluate, in the high-frequency limit  $ka \gg 1$  and  $kd \gg 1$ , the integral (70) by the saddle-point method. By

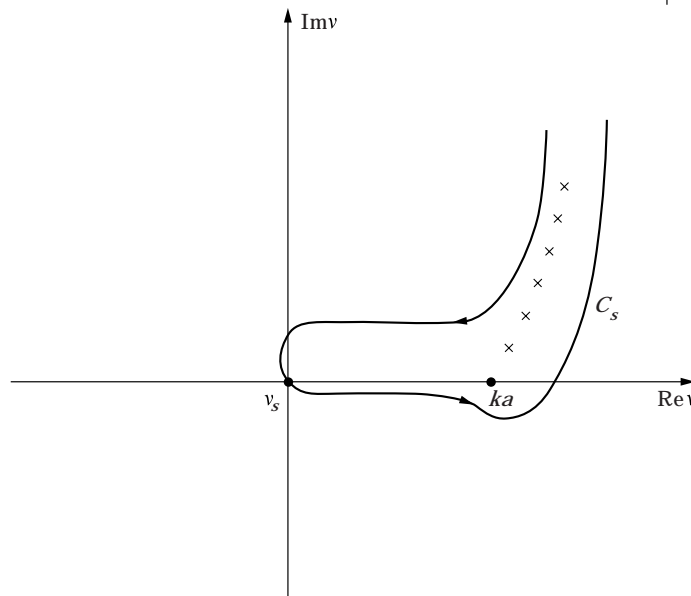


Figure 7. Contour  $C_s$  used to separate out the geometrically reflected wave.

inserting in the integral (70) the Debye asymptotic expansions for the Hankel functions [7]

$$H_\nu^{(1,2)}(z) \sim \sqrt{\frac{2}{\pi\sqrt{z^2 - \nu^2}}} \exp\left(\pm i\sqrt{z^2 - \nu^2} \mp i\nu \arccos \frac{\nu}{z} \mp i\frac{\pi}{4}\right), \quad (71)$$

the position of the saddle-point  $\nu_s$  can be determined. This gives  $\nu_s = 0$  and the integral (70) asymptotically reduces to

$$\frac{R_0}{2} \left( \sqrt{\frac{a}{2d-4a}} + \sqrt{\frac{a}{2d}} \right) \exp[ik(d-2a)]. \quad (72)$$

This contribution is obviously associated with the geometrical path described in Figure 6. More precisely,  $R_0$  denotes the direct reflection coefficient under normal incidence while the term  $k(d-2a)$  corresponds to the line integral of the propagation vector  $\mathbf{k}$  over the geometrical path. Now, by replacing the partial wave series in equation (63) by the purely geometrical contribution (72), one obtains from the condition

$$1 - \frac{R_0}{2} \left( \sqrt{\frac{a}{2d-4a}} + \sqrt{\frac{a}{2d}} \right) \exp[ik(d-2a)] = 0 \quad (73)$$

the locations of the  $A_1$  geometrical resonances in the complex  $ka$ -plane:

$$ka^{(A_1)}(p) = \frac{a}{d-2a} \left\{ (2p+1)\pi + i \ln \left[ \frac{R_0}{2} \left( \sqrt{\frac{a}{2d-4a}} + \sqrt{\frac{a}{2d}} \right) \right] \right\}, \quad p \in \mathbf{N}. \quad (74)$$

It should be noted that equation (74) has been obtained under restrictive hypotheses: the contributions of transmitted waves, internal reflected waves and surface waves have been neglected.

As far as equations (64–66) are concerned, slight changes in the previous calculations permits one to obtain the following high frequency approximations for the locations of the resonances in the complex  $ka$ -plane:

$$ka^{(A_2)}(p) = \frac{a}{d-2a} \left\{ 2p\pi + i \ln \left[ \frac{R_0}{2} \left( \sqrt{\frac{a}{2d-4a}} - \sqrt{\frac{a}{2d}} \right) \right] \right\}, \quad p \in \mathbf{N}, \quad (75)$$

$$ka^{(B_1)}(p) = \frac{a}{d-2a} \left\{ (2p+1)\pi + i \ln \left[ \frac{R_0}{2} \left( \sqrt{\frac{a}{2d-4a}} - \sqrt{\frac{a}{2d}} \right) \right] \right\}, \quad p \in \mathbf{N}, \quad (76)$$

$$ka^{(B_2)}(p) = \frac{a}{d-2a} \left\{ 2p\pi + i \ln \left[ \frac{R_0}{2} \left( \sqrt{\frac{a}{2d-4a}} + \sqrt{\frac{a}{2d}} \right) \right] \right\}, \quad p \in \mathbf{N}. \quad (77)$$

The exact values and high frequency approximations of complex resonances  $ka$  are presented in Tables 3 and 4 for Dirichlet boundary conditions ( $R_0 = 1$ ), and in Table 5 for Neumann boundary conditions ( $R_0 = -1$ ). Good agreement is found even for low frequencies. A physical interpretation has been provided for



TABLE 3

*Comparison between exact and high-frequency approximated resonances for Dirichlet boundary conditions (separation distance  $d = 6a$ )*

	Exact	Asymptotic
$A_1(p = 0)$	$0.7260 - 0.2612i$	$0.7854 - 0.2840i$
$B_2(p = 1)$	$1.5312 - 0.2747i$	$1.5708 - 0.2840i$
$A_1(p = 1)$	$2.3274 - 0.2788i$	$2.3562 - 0.2840i$
$B_2(p = 2)$	$3.1195 - 0.2815i$	$3.1416 - 0.2840i$
$A_1(p = 2)$	$3.9088 - 0.2832i$	$3.9270 - 0.2840i$
$B_2(p = 3)$	$4.6967 - 0.2841i$	$4.7124 - 0.2840i$
$A_1(p = 3)$	$5.4842 - 0.2846i$	$5.4978 - 0.2840i$
$B_2(p = 4)$	$6.2713 - 0.2850i$	$6.2832 - 0.2840i$
$A_1(p = 4)$	$7.0579 - 0.2853i$	$7.0686 - 0.2840i$
$B_2(p = 5)$	$7.8443 - 0.2855i$	$7.8540 - 0.2840i$
$A_1(p = 5)$	$8.6306 - 0.2857i$	$8.6394 - 0.2840i$
$B_2(p = 6)$	$9.4167 - 0.2858i$	$9.4248 - 0.2840i$
$A_1(p = 6)$	$10.2027 - 0.2859i$	$10.2102 - 0.2840i$
$B_2(p = 7)$	$10.9886 - 0.2860i$	$10.9956 - 0.2840i$
$A_1(p = 7)$	$11.7744 - 0.2861i$	$11.7810 - 0.2840i$
$B_2(p = 8)$	$12.5602 - 0.2861i$	$12.5664 - 0.2840i$
$A_1(p = 8)$	$13.3460 - 0.2862i$	$13.3518 - 0.2840i$
$B_2(p = 9)$	$14.1317 - 0.2862i$	$14.1372 - 0.2840i$
$A_1(p = 9)$	$14.9174 - 0.2862i$	$14.9226 - 0.2840i$
$B_2(p = 10)$	$15.7030 - 0.2863i$	$15.7080 - 0.2840i$
$A_1(p = 10)$	$16.4887 - 0.2863i$	$16.4934 - 0.2840i$
$B_2(p = 11)$	$17.2743 - 0.2863i$	$17.2788 - 0.2840i$
$A_1(p = 11)$	$18.0599 - 0.2863i$	$18.0642 - 0.2840i$
$B_2(p = 12)$	$18.8455 - 0.2864i$	$18.8496 - 0.2840i$
$A_1(p = 12)$	$19.6310 - 0.2864i$	$19.6350 - 0.2840i$
$B_2(p = 13)$	$20.4165 - 0.2864i$	$20.4204 - 0.2840i$

the resonances lying on the lines close to the real  $ka$  axis in terms of the phase-matching of geometrical rays along the closed path described in Figure 6.

## 5. CONCLUSION AND PERSPECTIVES

In the study of multiple scattering by two identical cylinders, the fields scattered by each cylinder are usually represented by means of two sums over partial waves, with unknown coefficients that are coupled through an infinite set of two linear, complex, algebraic equations. It has been shown that, by taking into account the symmetries of the scatterer, the use of group representation theory permits one to obtain an infinite set of four linear complex algebraic equations where the unknown coefficients are uncoupled. This feature greatly simplifies numerical calculations involved in this problem. This new approach can also be applied to transient situations and to more general problems of multiple scattering from an arbitrary number of cylinders when symmetries are present. Similarly, symmetry considerations can also be used to study sound scattering by a system of spheres. In the particular case of scattering by two

TABLE 4

*Comparison between exact and high-frequency approximated resonances for Dirichlet boundary conditions (separation distance  $d = 6a$ )*

	Exact	Asymptotic
$B_1(p = 0)$	0.6060 – 0.5774i	0.7854 – 0.8571i
$A_2(p = 1)$	1.5486 – 0.7068i	1.5708 – 0.8571i
$B_1(p = 1)$	2.4210 – 0.8287i	2.3562 – 0.8571i
$A_2(p = 2)$	3.0041 – 0.8459i	3.1416 – 0.8571i
$B_1(p = 2)$	3.8845 – 0.8158i	3.9270 – 0.8571i
$A_2(p = 3)$	4.7095 – 0.8447i	4.7124 – 0.8571i
$B_1(p = 3)$	5.4729 – 0.8780i	5.4978 – 0.8571i
$A_2(p = 4)$	6.2514 – 0.8491i	6.2832 – 0.8571i
$B_1(p = 4)$	7.0555 – 0.8502i	7.0686 – 0.8571i
$A_2(p = 5)$	7.8403 – 0.8630i	7.8540 – 0.8571i
$B_1(p = 5)$	8.6189 – 0.8577i	8.6394 – 0.8571i
$A_2(p = 6)$	9.4112 – 0.8544i	9.4248 – 0.8571i
$B_1(p = 6)$	10.1991 – 0.8595i	10.2102 – 0.8571i
$A_2(p = 7)$	10.9813 – 0.8594i	10.9956 – 0.8571i
$B_1(p = 7)$	11.7690 – 0.8568i	11.7810 – 0.8571i
$A_2(p = 8)$	12.5567 – 0.8588i	12.5664 – 0.8571i
$B_1(p = 8)$	13.3409 – 0.8595i	13.3518 – 0.8571i
$A_2(p = 9)$	14.1269 – 0.8581i	14.1372 – 0.8571i
$B_1(p = 9)$	14.9139 – 0.8587i	14.9226 – 0.8571i
$A_2(p = 10)$	15.6990 – 0.8594i	15.7080 – 0.8571i
$B_1(p = 10)$	16.4846 – 0.8587i	16.4934 – 0.8571i
$A_2(p = 11)$	17.2710 – 0.8589i	17.2788 – 0.8571i
$B_1(p = 11)$	18.0565 – 0.8595i	18.0642 – 0.8571i
$A_2(p = 12)$	18.8420 – 0.8591i	18.8496 – 0.8571i
$B_1(p = 12)$	19.6281 – 0.8590i	19.6350 – 0.8571i
$A_2(p = 13)$	20.4135 – 0.8594i	20.4204 – 0.8571i

spheres, the symmetry group involved is the continuous group  $D_{\infty h}$  [5] (the two-sphere scatterer is invariant (i) under rotations about the system axis, (ii) under reflection in the plane perpendicular to the system axis and which passes through the symmetry center of the system, (iii) under reflection in any plane passing through the axis of the system). It is then natural to solve this scattering problem by using the corresponding irreducible representations.

From symmetry considerations, the resonances of the two-cylinder scatterer have been partially classified. They lie in four distinct families associated with the four irreducible representations  $A_1$ ,  $A_2$ ,  $B_1$ ,  $B_2$  of the symmetry group of the scatterer  $\mathcal{C}_{2v}$ . From a mathematical point of view it would be useful to obtain a full classification of the two-cylinder scatterer resonances. With this aim in view, several techniques of Geometrical Theory of Diffraction and algebraic topology [17] could be initiated.

As a consequence of this approach, new physical effects are expected (splitting up of resonances and resonances of interaction between the two scatterers). It would be interesting to experimentally confirm these physical effects. It should be noted that in electromagnetism, in the context of microwave two-disc scattering,

TABLE 5

Comparison between exact and high-frequency approximated resonances for Neumann boundary conditions (separation distance  $d = 6a$ )

	Exact	Asymptotic
$B_2(p = 0)$	$0.8815 - 0.2065i$	$0.7854 - 0.2840i$
$A_1(p = 1)$	$1.7264 - 0.2561i$	$1.5708 - 0.2840i$
$B_2(p = 1)$	$2.3125 - 0.3221i$	$2.3562 - 0.2840i$
$A_1(p = 2)$	$3.1754 - 0.2545i$	$3.1416 - 0.2840i$
$B_2(p = 2)$	$3.9988 - 0.2778i$	$3.9270 - 0.2840i$
$A_1(p = 3)$	$4.7291 - 0.3331i$	$4.7124 - 0.2840i$
$B_2(p = 3)$	$5.5149 - 0.2720i$	$5.4978 - 0.2840i$
$A_1(p = 4)$	$6.3248 - 0.2800i$	$6.2832 - 0.2840i$
$B_2(p = 4)$	$7.0911 - 0.3082i$	$7.0686 - 0.2840i$
$A_1(p = 5)$	$7.8655 - 0.2799i$	$7.8540 - 0.2840i$
$B_2(p = 5)$	$8.6670 - 0.2812i$	$8.6394 - 0.2840i$
$A_1(p = 6)$	$9.4445 - 0.2985i$	$9.4248 - 0.2840i$
$B_2(p = 6)$	$10.2194 - 0.2838i$	$10.2102 - 0.2840i$
$A_1(p = 7)$	$11.0156 - 0.2823i$	$10.9956 - 0.2840i$
$B_2(p = 7)$	$11.7978 - 0.2937i$	$11.7810 - 0.2840i$
$A_1(p = 8)$	$12.5746 - 0.2857i$	$12.5664 - 0.2840i$
$B_2(p = 8)$	$13.3671 - 0.2832i$	$13.3518 - 0.2840i$
$A_1(p = 9)$	$14.1515 - 0.2911i$	$14.1372 - 0.2840i$
$B_2(p = 9)$	$14.9301 - 0.2866i$	$14.9226 - 0.2840i$
$A_1(p = 10)$	$15.7203 - 0.2839i$	$15.7080 - 0.2840i$
$B_2(p = 10)$	$16.5057 - 0.2895i$	$16.4934 - 0.2840i$
$A_1(p = 11)$	$17.2858 - 0.2871i$	$17.2788 - 0.2840i$
$B_2(p = 11)$	$18.0744 - 0.2844i$	$18.0642 - 0.2840i$
$A_1(p = 12)$	$18.8603 - 0.2885i$	$18.8496 - 0.2840i$
$B_2(p = 12)$	$19.6416 - 0.2873i$	$19.6350 - 0.2840i$
$A_1(p = 13)$	$20.4291 - 0.2849i$	$20.4204 - 0.2840i$

Kudrolli and Sridhar [18] have observed resonances corresponding to the  $A_2$  antisymmetric poles of the  $S$ -matrix. In acoustics, similar experiments in the case of the three-cylinder scatterer are in preparation [19].

## REFERENCES

1. J. W. YOUNG and J. C. BERTRAND 1975 *Journal of the Acoustical Society of America* **58**, 1190–1195. Multiple scattering by two cylinders.
2. L. D. LANDAU and E. M. LIFSHITZ 1975 *Quantum Mechanics*. Oxford: Pergamon.
3. P. GASPARD and S. A. RICE 1989 *Journal of Chemical Physics* **90**, 2255–2262. Exact quantization of the scattering from a classically chaotic repeller.
4. P. CVITANOVIĆ and B. ECKHARDT 1993 *Nonlinearity* **6**, 277–311. Symmetry decomposition of chaotic dynamics.
5. M. HAMERMESH 1989 *Group Theory and its Application to Physical Problems*. New York: Dover.
6. R. G. NEWTON 1982 *Scattering Theory in Waves and Particles*. New York: Springer Verlag.
7. M. A. ABRAMOWITZ and I. STEGUN (editors) 1964 *Handbook of Mathematical Functions*. New York: Dover.

8. J. J. FARAN 1951 *Journal of the Acoustical Society of America* **23**, 405–418. Sound scattering by solid cylinders and spheres.
9. R. D. DOOLITTLE, H. ÜBERALL and P. UGINČIUS 1968 *Journal of the Acoustical Society of America* **43**, 1–14. Sound scattering by elastic cylinders.
10. N. D. VEKSLER 1993 *Resonance Acoustic Spectroscopy*, Berlin: Springer-Verlag.
11. H. M. NUSSENZVEIG 1992 *Diffraction Effects in Semiclassical Scattering*. Cambridge: Cambridge University Press.
12. E. T. WHITTAKER and G. N. WATSON 1927 *A Course of Modern Analysis*. Cambridge: Cambridge University Press.
13. A. WIRZBA 1992 *Chaos* **2**, 77–83. Validity of the semiclassical periodic orbit approximation in the 2- and 3-disk problems.
14. G. N. WATSON 1918 *Proceedings of the Royal Society of London* **A95**, 83–99. The diffraction of electric waves by the earth.
15. P. J. DEBYE 1908 *Physik. Z.* **9**, 775–778. Das elektromagnetische Feld um einen Zylinder und die Theorie des Regenbogens.
16. D. BRILL and H. ÜBERALL 1970 *Journal of the Acoustical Society of America* **50**, 921–939. Acoustic waves transmitted through solid elastic cylinders.
17. C. NASH and S. SEN 1983 *Topology and Geometry for Physicists*. London: Academic Press.
18. A. KUDROLLI and S. SRIDHAR 1995 *Proceedings of the 4th Drexel Conference*. Singapore: World Scientific (to appear).
19. Y. DECANINI, A. FOLACCI E. FOURNIER and P. GABRIELLI, in preparation.